Article:
Xiao, K, Ge, T, Wu, X et al. (2021) Metagenomic and 14 C tracing evidence for autotrophic microbial CO2 fixation in paddy soils. Environmental Microbiology, 23 (2). pp. 924-933. ISSN: 1462-2912

https://doi.org/10.1111/1462-2920.15204

environmental microbiology
environmental microbiology reports

Metagenomic and 14C tracing evidence for autotrophic microbial CO2 fixation in paddy soils

Journal:	*Environmental Microbiology and Environmental Microbiology Reports*
Manuscript ID	EMI-2020-1232
Journal:	Environmental Microbiology
Manuscript Type:	EMI - Special Issue Article
Date Submitted by the Author:	30-Jul-2020
Complete List of Authors:	Xiao, Ke-Qing; University of Leeds, School of Earth and Environment Zhu, Yong-Guan; Chinese Academy of Sciences, Res Ctr Eco-environ Sci; Chinese Academy of Sciences, Institute of Urban Environment Ge, Tida; the Chinese Academy of Sciences (CAS), Institute of Subtropical Agriculture (ISA)
Keywords:	Autotrophic microbes, marker gene,, soil organic carbon, paddy soil

Metagenomic and ^{14}C tracing evidence for autotrophic microbial CO_2 fixation in paddy soils

Ke-Qing Xiao[1], Ti-Da Ge[2], Xiao-Hong Wu[3], Caroline L. Peacock[1], Zhen-Ke Zhu[2], Jingjing Peng[4], Peng Bao[5], Jin-Shui Wu[2], Yong-Guan Zhu[5 6 *]

[1]School of Earth and Environment, University of Leeds, Leeds LS2 9JT, UK; [2]Key Laboratory of Agro-ecological Processes in Subtropical Region & Changsha Research Station for Agricultural and Environmental Monitoring, Institute of Subtropical Agriculture, Chinese Academy of Sciences, Hunan 410125, China; [3]National Engineering Laboratory of Applied Technology for Forestry & Ecology in Southern China, Central South University of Forestry and Technology, Changsha 410004, Hunan, China; [4]College of Resources and Environmental Sciences, China Agricultural University, Beijing, 100193, China; [5]Key Lab of Urban Environment and Health, Institute of Urban Environment, Chinese Academy of Sciences, 1799 Jimei Road, Xiamen, 361021, China; [6]State Key Laboratory of Urban and Regional Ecology, Research Center for Eco-Environmental Sciences, Chinese Academy of Sciences, 18 Shuangqing Road, Beijing, 100085, China;

Running title: Autotrophic microbial CO_2 fixation in paddy soil

* Corresponding author
Address: State Key Laboratory of Urban and Regional Ecology, Research Center for Eco-Environmental Sciences, Chinese Academy of Sciences, 18 Shuangqing Road, Beijing, 100085, China.
Phone: 86-10-6293 6940
Fax: 86-10-6293 6940
Email: ygzhu@rcees.ac.cn

Originality-Significance Statement

The role of autotrophic carbon fixation in SOC formation is unclear to date. This study detects marker genes from all known autotrophic pathways in paddy soils for the first time using metagenomic analysis. ^{14}C-labelling experiment shows that autotrophic microbes are active and contribute significantly to the stable SOC pool. Our work highlights the importance of microbial CO_2 fixation to SOC accumulation in paddy soils.

Summary

Autotrophic carbon dioxide (CO_2) fixation by microbes is ubiquitous in the environment and potentially contributes to the soil organic carbon (SOC) pool. However, the multiple autotrophic pathways of microbial carbon assimilation and fixation in paddy soils remain poorly characterized. In this study, we combine metagenomic analysis with ^{14}C-labelling to investigate all known autotrophic pathways and CO_2 assimilation mechanisms in five typical paddy soils from southern China. Marker genes of six autotrophic pathways are detected in all soil samples, which are dominated by the *cbbL* genes (67-82%) coding the ribulose-bisphosphate carboxylase large chain in the Calvin cycle. These marker genes are associated with a broad range of phototrophic and chemotrophic genera. Significant amounts of ^{14}C-CO_2 are assimilated into SOC (74.3 to 175.8 mg ^{14}C kg^{-1}) and microbial biomass (5.2 to 24.1 mg ^{14}C kg^{-1}) after 45 days incubation, where more than 70% of ^{14}C-SOC was concentrated in the relatively stable humin fractions. These results show that paddy soil microbes contain the genetic potential for autotrophic carbon fixation spreading over broad taxonomic ranges, and can incorporate atmospheric carbon into organic components, which ultimately contribute to the stable SOC pool.

Introduction

Soil is the second largest pool of carbon on Earth, with 2000 Pg C in the form of

soil organic carbon (SOC) (Janzen, 2004). Soil organic carbon provides an important source of carbon for microbial growth (Schimel and Schaeffer, 2012; Lehmann and Kleber, 2015) and as part of soil organic matter supplies nutrients such as phosphorus, sulfur, calcium, magnesium, and trace elements (Kapkiyai et al., 1999; Dincher et al., 2020), which all contribute to the creation and maintenance of healthy soils that are able to perform a wide range of ecosystem services (Schmidt et al., 2011). The production and degradation of SOC also modulates the sequestration or release of CO_2 (Lal, 2008), and thus directly helps to regulate short-term climate and potentially mitigate against current climate change (Davidson and Janssens, 2006). Traditionally SOC is thought to derive mainly from plant detritus, but new research now shows that organic carbon from microbial sources might be the main contributor to SOC (Simpson et al., 2007; Kallenbach et al., 2016; Liang et al., 2017), with microbial necromass contributing up to 50-80% of SOC (Liang et al., 2019). This new work highlights the potential importance of soil microbes in producing and subsequently controlling the fate of SOC. Heterotrophic microbes have two critical but contrasting roles in controlling SOC: promoting release of C to the atmosphere through their catabolic production of CO_2, and preventing release of C to the atmosphere by transforming labile organic carbon into a more stable form through anabolism (Schimel and Schaeffer, 2012; Liang et al., 2017). Autotrophic microbes meanwhile can fix CO_2 from the atmosphere and synthesize this into microbial biomass (MBC) (Yuan et al., 2012b; Ge et al., 2013), which directly contributes to the SOC pool. Autotrophic metabolisms result in net C sequestration and can add to SOC in a continuously iterative process of cell generation, population growth and death (Liang and Balser, 2011; Liu et al., 2016). To date however, the role of autotrophic carbon fixation in SOC formation is unclear and remains to be elucidated.

The assimilation of CO_2 into organic material is quantitatively the most important biosynthetic process on Earth (Berg et al., 2007), as autotrophs generate the biomass on which all other organisms thrive (Thauer, 2007). Six autotrophic CO_2 fixation

pathways have been found in various environments to date: the Calvin cycle (Bassham et al., 1950), the reductive tricarboxylic acid (rTCA) cycle (Evans et al., 1966), the reductive acetyl-CoA pathway (Wood et al., 1986), the 3-hydroxypropionate / malyl-CoA cycle (Holo, 1989), and the 3-hydroxypropionate / 4-hydroxybutyrate and dicarboxylate / 4-hydroxybutyrate cycle (named together as the 4-hydroxybutyrate cycle) (Berg et al., 2007; Huber et al., 2008). The enzymes catalyzing difficult steps in a given pathway are usually conserved and act as key enzymes (Berg, 2011), and the corresponding coding genes, often named as marker genes (Lever, 2013), are commonly used in microbial ecological studies. For example, *cbbL* was used for ribulose 1,5-bisphosphate carboxylase/oxygenase (RubisCO) of the Calvin cycle (Alfreider et al., 2003; Selesi et al., 2005; Yuan et al., 2012a; Xiao et al., 2014b), *acl* for the ATP citrate lyase, *oorA* for 2-oxoglutarate: acceptor oxidoreductase in the rTCA pathway (Campbell et al., 2003; Campbell and Cary, 2004; Xiao et al., 2014a), and *hcd* for the 4-hydroxybutyryl-CoA dehydratase of both of the 4-hydroxybutyrate cycle (Zhang et al., 2010). Despite the discovery of these six pathways most studies only focus on one to two pathways (mainly the Calvin cycle), and there is a lack of comprehensive understanding of these pathways due to limitations of PCR primers, like bias or poor specificity. Metagenomics involves the direct sequencing of DNA from the environment and thus allows the examination of multiple biochemical pathways and associated processes, bypassing PCR primers, and so it is not limited to studying individual pieces of the metabolic puzzle (Venter et al., 2004; Mackelprang et al., 2011). With the development of high-throughput sequencing techniques and a dramatic drop of sequencing prices, diversity analysis based on metagenomes is now feasible, which can target all metabolic pathways in soil and does not rely on the specificity and coverage of the primers used (Liu et al., 2018; Ma et al., 2018). Moreover, metagenomics allows us to specifically analyze or explore functional groups, study gene function and even reconstruct whole microbial genome from complex environment samples (Tyson et al., 2004; Hultman et al., 2015;

Lam et al., 2015; Anantharaman et al., 2016; Metcalf et al., 2016).

Paddy soil is a common soil type in China and around the world, and is also an ideal model system for studying microbiological and biogeochemical processes (Liesack et al., 2000; Xiao et al., 2014a). In this study metagenomics and $^{14}CO_2$ labelling approaches are used to determine the genomic and geochemical potential of multiple autotrophic metabolisms in paddy soils to assimilate and fix atmospheric CO_2 into SOC. Soil physicochemical properties are used for statistical analyses to identify the key factors driving microbial CO_2 sequestration in paddy soils. With a systematic analysis of multiple autotrophic pathways and their activities in paddy soil, this work provides new insight into the role of autotrophic CO_2 fixation in SOC formation.

Results

Marker genes of different autotrophic pathways in paddy soil

Marker genes of six autotrophic pathways are detected in all samples (Fig. 1a): *cbbL* (Calvin cycle, coding ribulose-bisphosphate carboxylase large chain) 7.2-11.7 ppm, *aclA* (rTCA cycle, coding ATP-citrate lyase alpha-subunit) 0.8-1.6 ppm, *acsA* (reductive acetyl-CoA pathway, coding carbon-monoxide dehydrogenase catalytic subunit) 0.7-1.9 ppm, *accA* (3-hydroxypropionate/malyl-CoA cycle, coding acetyl-CoA carboxylase carboxyl transferase subunit alpha) 0.02-0.1 ppm, and *hcd* (4-hydroxybutyrate cycle, coding 4-hydroxybutyryl-CoA dehydratase) 0.2-1.8 ppm. The gene *cbbL* dominates (67-82%) in all samples, while *accA* is always the lowest (< 1%) (Fig. 1b).

Fig. 1

Table 1

Autotrophic microbes in paddy soils

Diverse microbes associated with marker genes are found for six autotrophic pathways in paddy soils (Tab. S1). There exists the highest diversity for *cbbL*, second for *acsA*, followed by *hcd* and *accA*, lowest for *aclA* (Tab. 1). In the Calvin cycle, there

are 80 associated genera, with 34 phototrophs (13-20%), 50 chemotrophs (69-78%) and 3 mixotrophs (both phototrophs and chemotrophs, 5-11%) - *Rhodopseudomonas palustris*, *Thiocystis violascens* and *Rhodobacter sphaeroides*. In the reductive citric acid cycle, these microbes are exclusively chemotrophs, dominated by *Nitrospira defluvii* (94-98%). In the reductive acetyl-CoA pathway, all 28 genera are chemotrophs, mainly anaerobes like sulfate-reducing bacteria, acetogenic bacteria and methanogens. All four genera involved in the 3-hydroxypropionate / malyl-CoA cycle are phototrophs- *Chloroflexus aggregans, Chloroherpeton thalassium, Erythrobacter litoralis* and *Roseiflexus* sp. RS-1. In the 4-hydroxybutyrate cycle, all detected genera involved belong to chemotrophic archaea, and are dominated by two ammonia oxidation archaea-*Nitrosopumilus koreensis* and *Nitrososphaera gargensis*. The co-occurrence patterns of autotrophic microbes of six pathways in paddy soils are shown by network inference (Fig. 2). The resulting network consists of 121 nodes and 871 edges with an average node connectivity of 14. The clustering coefficient is 0.65, and the modularity index is 0.5 (values > 0.4), suggesting that the network has a modular structure (Newman, 2006). Microbes associated with the Calvin cycle and the reductive acetyl-CoA pathway dominate the network owning to high diversity (Tab 1), and microbes associated with the same pathway are inclined to cluster together and have stronger connections.

Fig. 2

Evidence of ^{14}C-CO_2 assimilation by soil

After 45 days incubation the amounts of ^{14}C-CO_2 incorporated into the soil organic carbon (^{14}C-SOC) and microbial biomass (^{14}C-MBC) are determined. Significant amounts of ^{14}C-SOC and ^{14}C-MBC are recovered from soils incubated under $^{14}CO_2$ atmosphere (Fig. 3a). The amounts of ^{14}C-SOC and ^{14}C-MBC range from 74.3 (JX) to 175.8 (LZ) mg kg^{-1} and from 5.2 (YT) to 24.1 (TY-G) mg kg^{-1}, respectively, and ^{14}C-MBC / ^{14}C-SOC varies between 3.4% (LZ) and 24.9% (TY-G). The differences between soils in terms of incorporation into SOC and MBC vary

significantly between some paddy soils (P < 0.05). The calculated rates of CO_2 assimilation into SOC in paddy soils are 34.2-62.2 mg C m^{-2} d^{-1} (Fig. 3b). The total Fe, clay and sand contents, and abundances of *cbbL* are significantly (P < 0.05) correlated with the amounts of ^{14}C-SOC in paddy soils (Tab. 2).

Fig.3

Table 2.

Fractionations of soil organic carbon (SOC)

The distribution of SOC and ^{14}C-SOC in paddy soils after 45 days incubation are characterized by either physical separation into different sizes or chemical separation into different fractions based on solubility in alkali or acid. Soil organic carbon and ^{14}C-SOC are mainly detected in micro-aggregates (0.25–0.053 mm) and silt and clay (< 0.053 mm) except for LZ and TY-B, while ^{14}C-SOC tends to concentrate in macro-aggregates compared to the small proportions in bulk soil (Fig. 4a). For the chemical fractions, humins (HM) and fulvic acids (FA) dominate in bulk SOC, while ^{14}C-SOC concentrates mainly in HM for all samples (> 70%) (Fig. 4b)

Fig. 4

Discussion

Marker genes and microbes involved in six autotrophic pathways for atmospheric CO_2 fixation in soils are detected and compared systematically for the first time in paddy soils using metagenomic analyses. These genes are as abundant as other genes involved in carbon, nitrogen, and sulfur cycling, arsenic metabolism, and antibiotic resistance, etc. (Mackelprang et al., 2011; Xiao et al., 2016b; Xiao et al., 2016a; Su et al., 2017). Results show that the Calvin cycle is the most abundant pathway in paddy soils according to marker genes analysis (Fig. 1), while other studies show that the reductive citric cycle dominates in desert soils (Liu et al., 2018), and the reverse tricarboxylic acid cycle dominates in free-fiving microorganisms at deep-sea hydrothermal vents (Campbell and Cary, 2004). These results indicate the niche preference of different autotrophic metabolisms. The genera carrying *cbbL* are

similar to previous studies using the regular sanger-sequencing methods (Yuan et al., 2012b; Xiao et al., 2014b), with phototrophs dominated by cyanobacteria, and chemoautotrophs by microbes involved in sulfur, ammonia and iron oxidation (Tab. S1). Results here also show that the marker genes associated with alternative autotrophic pathways, other than the Calvin cycle, are ubiquitously found in paddy soils (Fig. 1). There exists varied redox conditions in paddy soils, due to different spatial and temporal conditions like rhizosphere vs. bulk soil, flooded vs. drained conditions (Liesack et al., 2000), so genes and microbes associated with the rTCA (mainly in micro-aerophiles and anaerobes) and especially the reductive acetyl-CoA pathways (only in anaerobes) also exist in our samples. The 3-hydroxypropionate / malyl-CoA cycle is poorly represented in the paddy soils, which is known to have limited distribution due to the high energy cost involved in CO_2 assimilation (Berg, 2011). An important characteristic of this pathway is that it allows the co-assimilation of numerous organic compounds, making it suitable for the mixotrophic microbes (Zarzycki and Fuchs, 2011). The 4-hydroxypropionate cycle is only recently proposed (Berg et al., 2007; Huber et al., 2008) and only found in archaea to date, however this pathway is important in soils as it is lately found to be used by the *Thaumarchaea*, a main ammonia oxidizer in soil (Zhang et al., 2010), as the data here also shows (Tab. S1).

Results here show that autotrophic microbes are active and assimilate CO_2 into MBC in paddy soils, which ultimately contributes to SOC (Fig. 3). In the work here significant $^{14}CO_2$ assimilation is detected only when soils are incubated in the light, with almost no uptake when incubated in the dark (Yuan et al., 2012b; Ge et al., 2013), suggesting that the microbial CO_2 assimilation processes are driven primarily by autotrophs (including photo and chemoautotrophic microbes) in paddy soil. After 45 days incubation, 0.4-1.4% SOC and 6.7-15.1% MBC (data not shown) are labelled by ^{14}C, corresponding to turnover times of 8.8-30.3 years for SOC and 0.8-1.8 years for MBC, assuming a net autotrophic metabolism in paddy soil. This shows that OC from

microbial CO_2 fixation can sustain a relatively fast turnover of microbial biomass in paddy soil, but that this C tends to become more stable after partitioning into SOC. In particular results show that more than 70% of the ^{14}C-SOC concentrates in humins (Fig. 4b), which are thought to be the least available for microbial degradation as they are usually found to be strongly associated with soil minerals (Calace et al., 2007). In support of this assertion there are significant positive correlations between clay contents, total Fe and ^{14}C-SOC in the paddy soils (Tab. 2), which is in line with the growing evidence for the role of abiotic mechanisms, involving mineral sequestration of SOC, in controlling SOC persistence in (Totsche et al., 2018; Hemingway et al., 2019), with clay and iron oxides as the main minerals involved (Schweizer et al., 2019; Wan et al., 2019). Soil microbes are also known to excrete extracellular polymeric substance (EPS) (Cai et al., 2019), which play an important role in binding to soil minerals and thus creating stable soil aggregates (Cai et al., 2018; Lin et al., 2018) that help stabilize organic carbon in soil (Totsche et al., 2018). In our data, ^{14}C-SOC was distributed in different sizes of soil aggregate (Fig. 4a), suggesting that the organic carbon from autotrophic CO_2 fixation contributes to the formation of soil aggregates (Paerl and Priscu, 1998; Luo et al., 2019). It is also noteworthy that organic carbon synthesized by autotrophs can be processed by heterotrophic microbes and even virus and then transformed into MBC or SOC. For example, virus in soil can lyse cell of autotrophs, releasing organics, which can be used by heterotrophs, or transformed into more stable organic carbon (Liang and Balser, 2011; Schimel and Schaeffer, 2012; Liang et al., 2019; Bi et al., 2020). Taken together multiple processes (like mineral protection, aggregation, and microbial transformation, etc.) can strengthen the contribution of autotrophic metabolism to SOC accumulation in paddy soils.

Paddy soil proves to be a reservoir of multiple autotrophic metabolisms (Fig. 1 and Tab. S1) and thus is an ideal natural laboratory for their study. In particular there exists periodically changing redox conditions (oxic / anoxic) in paddy soil (Liesack et

al., 2000; Ge et al., 2012), so these might prove to be ideal environments to study the role of oxygen on the evolution and diversification of autotrophic pathways, where oxygen is thought to be one of the main controlling factors of these processes (Thauer, 2007; Ward and Shih, 2019). Autotrophic pathways emerged and diversified as a result of oxygenation events during Earth history and key enzymes of many autotrophic pathways show different sensitivities to oxygen, which directly determines their distribution among microbes and in different environments (Berg, 2011). Some microbes have more than one autotrophic pathway, like *Thioflavicoccus mobilis* which possesses the genes for both the Calvin cycle and rTCA pathway (Tab. S1) (Markert et al., 2007; Rubin-Blum et al., 2019) and the conditional usage of different CO_2 fixation pathways can be advantageous for this bacterial symbiont under fluctuating redox conditions (Berg, 2011). The interplay between the Calvin cycle and rTCA cycle in this bacterium may contribute to the high efficiency of carbon fixation under similar conditions in paddy soils as well. Lastly, *Geobacter sulfurreducens*, a common heterotrophic bacteria in paddy soil, is found to have a hidden chemolithoautotrophic metabolism and can reduce CO_2 via the rTCA cycle after adaption in chemolithoautotrophic growth medium containing Fe (III) and formate (Zhang et al., 2020), implying hidden autotrophic potential in other common microbes. Therefore a better understanding of these autotrophic metabolisms is needed, which is also critical for management practices to increase SOC in the context of climate change (Sá et al., 2017; Soussana et al., 2019).

In summary marker genes of six autotrophic pathways are detected in all paddy samples using metagenomic analysis, which are dominated by the *cbbL* genes in the Calvin cycle. Autotrophic microbes are active and assimilate 74.3 to 175.8 mg ^{14}C kg^{-1} into SOC and 5.2 to 24.1 mg ^{14}C kg^{-1} into MBC after 45 days incubation. Autotrophic microbes contribute significantly to the stable organic carbon pool, where more than 70% of ^{14}C-SOC was concentrated in the relatively stable humin fractions. Our work highlights the importance of microbial CO_2 fixation to SOC accumulation in paddy

soils.

Experimental procedures

Soil sampling and DNA extraction

Top soil (0-20 cm) from five distinct sites in south China, Leizhou in Guangdong Province (LZ), Jiaxing in Zhejiang Province(JX), Yingtan in Jiangxi Province (YT), Gushi in Taoyuan (TY-G) and Baodongyu in Taoyuan (TY-B) in Hunan Province were obtained. Rice is the main crop in these areas and diverse paddy soils develop from different parent materials (Fig. S1). Physiochemical characteristics of the collected soils are detailed in previous studies (Xiao et al., 2014b). To obtain sufficient DNA from each of the five soil samples for metagenomic sequencing, DNA was extracted from the five paddy soils (in duplicates) using the MoBio PowerSoil kit (MOBIO) according to the manufacturer's protocol. DNA yields of 10 samples were between 1.0 and 2.5 ug, as quantified using the Quant-iT Picogreen dsDNA HS assay kit (Invitrogen) according to the manufacturer's manual.

Sequencing and reads annotation

DNA library preparation was performed according to the Illumina TruSeq DNA sample preparation protocol. Each DNA sample was mechanically sheared by Covaris M220 (Covaris). Libraries were then size-selected to about 300 bp. Fragments were quantified using Agilent 2100 High Sensitivity DNA Assay (Agilent). Sequencing was performed at Majorbio, Inc., Shanghai, China using Illumina Hiseq 2000 (Illumina) generating 2 x 101 bp paired end reads. BBtools (https://sourceforge.net/projects/bbmap/) was used to remove trace contaminants. Raw reads were trimmed of adaptors and low quality reads using Sickle (https://github.com/najoshi/sickle) and Seqprep (https://github.com/jstjohn/SeqPrep) at default parameters, respectively. Low quality reads that contained ambiguous nucleotides or had a quality value lower than 20 were removed (Chen et al., 2013). The chimeric sequences were filtered out by UCHIME (Edgar et al., 2011). A total of

750,385,006 clean reads were generated across all 10 samples with an average of 75,038,500 reads per sample. Data are available at the NCBI Short Read Archive under accession number SRA023560.

To facilitate the annotation speed, nucleotide and amino acid sequences of targeted KEGG Orthologies (KO) of five marker genes (K01601 *cbbL*, K15230 *aclA*, K00198 *acsA*, K01962 *accA* and K14534 *hcd*) involved in microbial CO_2 fixation pathways were extracted from the KEGG database and used as a subject database for analysis. These sequences were reviewed with high quality and strictness, which had to be confirmed by case studies already, and only the complete open reading frame (ORF) sequences were included. The local BLASTX programs were employed to align clean reads of each data set to the subject database with e value 1 x 10^{-5}, similarity > 90%, and aligned amino acids length > 25 (Cai et al., 2013; Xiao et al., 2016a). The relative abundance of each gene was determined as hit numbers divided by total number of reads (ppm, one read in one million reads). Marker genes associated microbes were defined as microbes of aligned sequenced and summarized at genus level. Microbial community diversity was quantified using Shannon–Weiner diversity index (H, e as bases), as listed in Table 1. Similarity matrix of microbial co-occurrence network was calculated using Spearman correlation in R (https://personality-project.org/r/psych). Co-occurrence network was visualized by Gephi (Bastian et al., 2009), with cut-off values correlation coefficient > 0.6 and false discovery rate (FDR) corrected ($P < 0.01$).

Incubation with ^{14}C-labeled CO_2

One set of microcosms of the five soils, each with four replicates, were prepared by weighing 500 g (on an oven-dried basis) of fresh soil into PVC plastic tubes (20 cm diameter × 15 cm height). All PVC columns were incubated in a growth chamber (80 × 200 cm, height 120 cm) for 45 days with continuous ^{14}C-CO_2 labeling as described previously (Ge et al., 2013; Wu et al., 2015). The ^{14}C-CO_2 was generated by forcing a ^{14}C-Na_2CO_3 solution (1.0 M, a radioactivity of 1.68 × 10^4 Bq μg^{-1} C) into an acid bath

(HCl, 2 M) and giving a concentration from 360 and 380 μL L^{-1} (Shsen-QZD, Qingdao, China). Two temperature humidity sensors (SNT-96S, Qingdao, China) were installed: one inside the chamber, and another in the surrounding rice field in the open air. An air-conditioning system was used to control the temperature inside the chamber within 1°C from ambient temperature in the field (outside). Two fans continuously circulated the atmosphere in the growth chamber. The incubation chamber system was placed outdoors in order to maintain natural exposure to sunlight (Ge et al., 2014), as there was almost no uptake of $^{14}CO_2$ when incubated in the dark (Yuan et al., 2012b; Ge et al., 2013). The paddy soils were permanently flooded (2-3 cm water layer) by the addition of sterile distilled water as required during the incubation span. At the end of the 45 days incubation, soils were removed from the microcosms, mixed thoroughly then divided into two separate portions. One portion was oven-dried at 70°C to a constant weight to determine the amount of ^{14}C-SOC fixed from $^{14}CO_2$, and the other was stored at 4°C to determine ^{14}C-MBC. The synthesis rates (RS) of ^{14}C-SOC (RS, g C m^{-2} d^{-1}) were calculated using the formula: RS = ^{14}C-SOC * (1/(3.14* $(D/2)^2$)) / T, where D represents the internal diameter of the container (m) and T, the incubation time (45 d) respectively.

Soil partition and ^{14}C radioactivity analysis

Soil aggregate size fractionation was performed by the wet sieving method (Gale et al., 2000). Briefly, air-dried soil was sieved through 8 mm mesh and was gently crumbled manually to approximately 2 mm pieces. A 100 g soil sample was transferred to two sieves (0.25 and 0.053 mm) and shaken for 5 min. Subsequently, macro-aggregates (2–0.25 mm) and micro-aggregates (0.25–0.053 mm) were collected from the 0.25 mm and 0.053 mm sieves, respectively. The remaining material that passed through the 0.053 mm sieve was classified as silt and clay (< 0.053 mm). All size fractions were dried at 70 °C, weighed, and stored for ^{14}C analysis. The extraction of SOC pools from air-dried soil was performed using the methodology recommended by the International Humic Substances Society (IHSS), using

363 NaOH-$Na_4P_2O_7 \cdot 10H_2O$ (0.1 M, pH = 13) as the extraction agent (Swift, 1996). Three
364 fractions were separated from 5 g soil samples based on their solubility in alkaline and
365 acid solutions, and separated into three fractions: (a) alkali- and acid-extractable fulvic
366 acids (FAs); (b) alkali-extractable, acid non-extractable humic acids (HAs); and (3)
367 alkali and acid non-extractable humin (HM). For ^{14}C analysis, 3.0 ml 2.5 M HCl was
368 added and mixed with 1.50 g of soil (sieved with a mesh < 0.149 mm) (v: w = 2: 1) in
369 Dophin tubes for 24 hours to remove inorganic carbon (such as $CaCO_3$ in soil
370 samples). Then, the aliquots were washed twice with 3.0 ml H_2O to remove any
371 remaining HCl (Theis et al., 2007) before measuring ^{14}C-SOC. After that, 1.50 g
372 inorganic carbon-removed soil was digested with a mixture of $K_2Cr_2O_7$ and
373 concentrated H_2SO_4–H_3PO_4, as described by Ge *et al.* (2013). ^{14}C-MBC measurement
374 was performed based on the fumigation-extraction method and was determined using
375 K_2SO_4 extracts (Wu and O'Donnell, 1997), and the ^{14}C radioactivity was measured
376 using an automated liquid scintillation counter (LS-6500, Beckman, Germany). The
377 ^{14}C-SOC and ^{14}C-MBC amounts were calculated according to the procedure
378 described by Ge *et al.* (2013). Full details are given in previous studies of the
379 co-author groups (Ge et al., 2013; Wu et al., 2014; Wu et al., 2015).

380 **Statistical analysis**

381 All data are expressed as the mean ± standard error (or deviation). Differences
382 between means were evaluated by one-way analysis of variance (ANOVA) after
383 normal distribution test. Correlation analyses were carried out using the Spearman
384 correlation method. Significance was defined at the 0.05 level unless otherwise stated.
385 All analyses were performed using SPSS 18.0.

386

387 **Acknowledgements**

388 This work was supported by National Science Foundation of China (Grant 41090282,
389 Grant 41977038 and Grant 41950410565), Key Projects of Natural Science
390 Foundation of China (Grant 41090280), Hunan Province Base for Scientific and

Technological Innovation Cooperation (2018WK4012), the Youth Innovation Team Project of Institute of Subtropical Agriculture, Chinese Academy of Sciences (2017QNCXTD_GTD), National Natural Science Foundation of Hunan Province (2019JJ10003 and 2019JJ30028), and NERC Highlight Topic Grant (NE/S004963/1 Locked Up). In addition, this research project has received funding from the European Research Council (ERC) under the European Union's Horizon 2020 research and innovation programme (Grant agreement No. 725613 MinOrg).

Competing of Interests

The authors declare no competing interests.

References

Alfreider, A., Vogt, C., Hoffmann, D., and Babel, W. (2003) Diversity of ribulose-1,5-bisphosphate carboxylase/oxygenase large-subunit genes from groundwater and aquifer microorganisms. *Microbial Ecol* **45**: 317-328.

Anantharaman, K., Brown, C.T., Hug, L.A., Sharon, I., Castelle, C.J., Probst, A.J. et al. (2016) Thousands of microbial genomes shed light on interconnected biogeochemical processes in an aquifer system. *Nat Commun* **7**: 13219.

Bassham, J.A., Benson, A.A., and Calvin, M. (1950) The pathway of carbon in photosynthesis. *J Biol Chem* **185**: 781-788.

Bastian, M., Heymann, S., and Jacomy, M. (2009) *Gephi: An Open Source Software for Exploring and Manipulating Networks*.

Berg, I.A. (2011) Ecological aspects of the distribution of different autotrophic CO_2 fixation pathways. *Appl Environ Microbiol* **77**: 1925-1936.

Berg, I.A., Kockelkorn, D., Buckel, W., and Fuchs, G. (2007) A 3-hydroxypropionate/4-hydroxybutyrate autotrophic carbon dioxide assimilation pathway in archaea. *Science* **318**: 1782-1786.

Bi, L., Yu, D.T., Du, S., Zhang, L.M., Zhang, L.Y., Wu, C.F. et al. (2020) Diversity and potential biogeochemical impacts of viruses in bulk and rhizosphere soils. *Environ Microbiol* **n/a**.

Cai, L., Yu, K., Yang, Y., Chen, B.-w., Li, X.-d., and Zhang, T. (2013) Metagenomic exploration reveals high levels of microbial arsenic metabolism genes in activated sludge and coastal sediments. *Appl Microbiol Biol* **97**: 9579-9588.

Cai, P., Lin, D., Peacock, C.L., Peng, W., and Huang, Q. (2018) EPS adsorption to goethite: Molecular level adsorption mechanisms using 2D correlation spectroscopy. *Chem Geol* **494**: 127-135.

Cai, P., Sun, X., Wu, Y., Gao, C., Mortimer, M., Holden, P.A. et al. (2019) Soil biofilms: microbial interactions, challenges, and advanced techniques for ex-situ characterization. *Soil Ecology Letters* **1**: 85-93.

Calace, N., Petronio, B.M., Persia, S., Pietroletti, M., and Pacioni, D. (2007) A new analytical approach for humin determination in sediments and soils. *Talanta* **71**: 1444-1448.

Campbell, B.J., and Cary, S.C. (2004) Abundance of reverse tricarboxylic acid cycle genes in free-living microorganisms at deep-sea hydrothermal vents. *Appl Environ Microbiol* **70**: 6282-6289.

Campbell, B.J., Stein, J.L., and Cary, S.C. (2003) Evidence of chemolithoautotrophy

437 in the bacterial community associated with *Alvinella pompejana*, a hydrothermal vent
438 polychaete. *Appl Environ Microbiol* **69**: 5070-5078.
439 Chen, B., Yang, Y., Liang, X., Yu, K., Zhang, T., and Li, X. (2013) Metagenomic
440 profiles of antibiotic resistance genes (ARGs) between human impacted estuary and
441 deep ocean sediments. *Environ Sci Technol* **47**: 12753-12760.
442 Davidson, E.A., and Janssens, I.A. (2006) Temperature sensitivity of soil carbon
443 decomposition and feedbacks to climate change. *Nature* **440**: 165-173.
444 Dincher, M., Calvaruso, C., and Turpault, M.-P. (2020) Major element residence times
445 in humus from a beech forest: The role of element forms and recycling. *Soil Biol*
446 *Biochem* **141**: 107674.
447 Edgar, R.C., Haas, B.J., Clemente, J.C., Quince, C., and Knight, R. (2011) UCHIME
448 improves sensitivity and speed of chimera detection. *Bioinformatics* **27**: 2194-2200.
449 Evans, M.C., Buchanan, B.B., and Arnon, D.I. (1966) A new ferredoxin-dependent
450 carbon reduction cycle in a photosynthetic bacterium. *Proc Natl Acad Sci U S A* **55**:
451 928-934.
452 Gale, W.J., Cambardella, C.A., and Bailey, T.B. (2000) Root-derived carbon and the
453 formation and stabilization of aggregates. *Soil Sci Soc Am J* **64**: 201-207.
454 Ge, T., Liu, C., Yuan, H., Zhao, Z., Wu, X., Zhu, Z. et al. (2014) Tracking the
455 photosynthesized carbon input into soil organic carbon pools in a rice soil fertilized
456 with nitrogen. *Plant Soil* **392**: 17-25.
457 Ge, T., Yuan, H., Zhu, H., Wu, X., Nie, S.a., Liu, C. et al. (2012) Biological carbon
458 assimilation and dynamics in a flooded rice – Soil system. *Soil Biol Biochem* **48**:

459 39-46.

460 Ge, T., Wu, X., Chen, X., Yuan, H., Zou, Z., Li, B. et al. (2013) Microbial phototrophic
461 fixation of atmospheric CO2 in China subtropical upland and paddy soils. *Geochim*
462 *Cosmochim Acta* **113**: 70-78.

463 Hemingway, J.D., Rothman, D.H., Grant, K.E., Rosengard, S.Z., Eglinton, T.I., Derry,
464 L.A., and Galy, V.V. (2019) Mineral protection regulates long-term global preservation
465 of natural organic carbon. *Nature* **570**: 228-231.

466 Holo, H. (1989) Chloroflexus aurantiacus secretes 3-hydroxypropionate, a possible
467 intermediate in the assimilation of CO2 and acetate. *Arch Microbiol* **151**: 252-256.

468 Huber, H., Gallenberger, M., Jahn, U., Eylert, E., Berg, I.A., Kockelkorn, D. et al.
469 (2008) A dicarboxylate/4-hydroxybutyrate autotrophic carbon assimilation cycle in the
470 hyperthermophilic Archaeum Ignicoccus hospitalis. *Proc Natl Acad Sci U S A* **105**:
471 7851-7856.

472 Hultman, J., Waldrop, M.P., Mackelprang, R., David, M.M., McFarland, J., Blazewicz,
473 S.J. et al. (2015) Multi-omics of permafrost, active layer and thermokarst bog soil
474 microbiomes. *Nature* **521**: 208-212.

475 Janzen, H.H. (2004) Carbon cycling in earth systems—a soil science perspective. *Agr*
476 *Ecosyst Environ* **104**: 399-417.

477 Kallenbach, C.M., Frey, S.D., and Grandy, A.S. (2016) Direct evidence for
478 microbial-derived soil organic matter formation and its ecophysiological controls. *Nat*
479 *Commun* **7**: 13630.

480 Kapkiyai, J.J., Karanja, N.K., Qureshi, J.N., Smithson, P.C., and Woomer, P.L. (1999)

481 Soil organic matter and nutrient dynamics in a Kenyan nitisol under long-term fertilizer
482 and organic input management. *Soil Biol Biochem* **31**: 1773-1782.
483 Lal, R. (2008) Carbon sequestration. *Philos T Roy Soc B* **363**: 815-830.
484 Lam, K.N., Cheng, J., Engel, K., Neufeld, J.D., and Charles, T.C. (2015) Current and
485 future resources for functional metagenomics. *Front Microbiol* **6**.
486 Lehmann, J., and Kleber, M. (2015) The contentious nature of soil organic matter.
487 *Nature* **528**: 60.
488 Lever, M.A. (2013) Functional gene surveys from ocean drilling expeditions – a review
489 and perspective. *FEMS Microbiol Ecol* **84**: 1-23.
490 Liang, C., and Balser, T.C. (2011) Microbial production of recalcitrant organic matter
491 in global soils: implications for productivity and climate policy. *Nat Rev Micro* **9**: 75-75.
492 Liang, C., Schimel, J.P., and Jastrow, J.D. (2017) The importance of anabolism in
493 microbial control over soil carbon storage. *Nat Microbiol* **2**: 17105.
494 Liang, C., Amelung, W., Lehmann, J., and Kastner, M. (2019) Quantitative
495 assessment of microbial necromass contribution to soil organic matter. *Glob Chang*
496 *Biol* **25**: 3578-3590.
497 Liesack, W., Schnell, S., and Revsbech, N.P. (2000) Microbiology of flooded rice
498 paddies. *FEMS Microbiol Rev* **24**: 625-645.
499 Lin, D., Cai, P., Peacock, C.L., Wu, Y., Gao, C., Peng, W. et al. (2018) Towards a
500 better understanding of the aggregation mechanisms of iron (hydr)oxide nanoparticles
501 interacting with extracellular polymeric substances: Role of pH and electrolyte
502 solution. *Sci Total Environ* **645**: 372-379.

503 Liu, J., Kong, W., Zhang, G., Khan, A., Guo, G., Zhu, C. et al. (2016) Diversity and
504 succession of autotrophic microbial community in high-elevation soils along
505 deglaciation chronosequence. *FEMS Microbiol Ecol* **92**.
506 Liu, Z., Sun, Y., Zhang, Y., Feng, W., Lai, Z., Fa, K., and Qin, S. (2018) Metagenomic
507 and 13C tracing evidence for autotrophic atmospheric carbon absorption in a semiarid
508 desert. *Soil Biol Biochem* **125**: 156-166.
509 Luo, Y., Zhu, Z., Liu, S., Peng, P., Xu, J., Brookes, P. et al. (2019) Nitrogen
510 fertilization increases rice rhizodeposition and its stabilization in soil aggregates and
511 the humus fraction`. *Plant Soil* **445**: 125-135.
512 Ma, B., Zhao, K., Lv, X., Su, W., Dai, Z., Gilbert, J.A. et al. (2018) Genetic correlation
513 network prediction of forest soil microbial functional organization. *ISME J* **12**:
514 2492-2505.
515 Mackelprang, R., Waldrop, M.P., DeAngelis, K.M., David, M.M., Chavarria, K.L.,
516 Blazewicz, S.J. et al. (2011) Metagenomic analysis of a permafrost microbial
517 community reveals a rapid response to thaw. *Nature* **480**: 368-371.
518 Markert, S., Arndt, C., Felbeck, H., Becher, D., Sievert, S.M., Hügler, M. et al. (2007)
519 Physiological proteomics of the uncultured endosymbiont of *Riftia pachyptila*. *Science*
520 **315**: 247.
521 Metcalf, J.L., Xu, Z.Z., Weiss, S., Lax, S., Van Treuren, W., Hyde, E.R. et al. (2016)
522 Microbial community assembly and metabolic function during mammalian corpse
523 decomposition. *Science* **351**: 158-162.
524 Newman, M.E.J. (2006) Modularity and community structure in networks. *Proc Natl*

Acad Sci U S A **103**: 8577.

Paerl, H.W., and Priscu, J.C. (1998) Microbial phototrophic, heterotrophic, and diazotrophic activities associated with aggregates in the lermanent ice cover of Lake Bonney, Antarctica. *Microbial Ecol* **36**: 221-230.

Rubin-Blum, M., Dubilier, N., and Kleiner, M. (2019) Genetic evidence for two carbon fxation pathways (the Calvin-Benson-Bassham cycle and the reverse tricarboxylic acid cycle) in symbiotic and free-Living bacteria. *mSphere* **4**: e00394-00318.

Sá, J.C.d.M., Lal, R., Cerri, C.C., Lorenz, K., Hungria, M., and de Faccio Carvalho, P.C. (2017) Low-carbon agriculture in South America to mitigate global climate change and advance food security. *Environ Int* **98**: 102-112.

Schimel, J., and Schaeffer, S. (2012) Microbial control over carbon cycling in soil. *Front Microbiol* **3**.

Schmidt, M.W.I., Torn, M.S., Abiven, S., Dittmar, T., Guggenberger, G., Janssens, I.A. et al. (2011) Persistence of soil organic matter as an ecosystem property. *Nature* **478**: 49-56.

Schweizer, S.A., Bucka, F.B., Graf-Rosenfellner, M., and Kögel-Knabner, I. (2019) Soil microaggregate size composition and organic matter distribution as affected by clay content. *Geoderma* **355**: 113901.

Selesi, D., Schmid, M., and Hartmann, A. (2005) Diversity of green-like and red-like ribulose-1,5-bisphosphate carboxylase/oxygenase large-subunit genes (*cbbL*) in differently managed agricultural soils. *Appl Environ Microbiol* **71**: 175-184.

Simpson, A.J., Simpson, M.J., Smith, E., and Kelleher, B.P. (2007) Microbially derived

547 inputs to soil organic matter: are current estimates too low? *Environ Sci Technol* **41**:
548 8070-8076.
549 Soussana, J.-F., Lutfalla, S., Ehrhardt, F., Rosenstock, T., Lamanna, C., Havlík, P. et
550 al. (2019) Matching policy and science: Rationale for the '4 per 1000 - soils for food
551 security and climate' initiative. *Soil Till Res* **188**: 3-15.
552 Su, J.-Q., Xia, Y., Yao, H.-Y., Li, Y.-Y., An, X.-L., Singh, B.K. et al. (2017)
553 Metagenomic assembly unravel microbial response to redox fluctuation in acid sulfate
554 soil. *Soil Biol Biochem* **105**: 244-252.
555 Swift, R.S. (1996) Organic matter characterization. In *Methods of Soil Analysis*. D.L.
556 Sparks, A.L.P., P.A. Helmke, R.H. Loeppert, P. N. Soltanpour, M. A. Tabatabai,
557 C. T. Johnston, M. E. Sumner (ed). No. 5, Madison, WI, USA: Soil Science Society of
558 America.
559 Thauer, R.K. (2007) A fifth pathway of carbon fixation. *Science* **318**: 1732-1733.
560 Theis, D.E., Jaeggi, M., Aeschlimann, D., Blum, H., Frossard, E., and Siegwolf,
561 R.T.W. (2007) Dynamics of soil organic matter turnover and soil respired CO_2 in a
562 temperate grassland labelled with ^{13}C. *Eur J Soil Sc* **58**: 1364-1372.
563 Totsche, K.U., Amelung, W., Gerzabek, M.H., Guggenberger, G., Klumpp, E., Knief,
564 C. et al. (2018) Microaggregates in soils. *J Plant Nutr Soil Sci* **181**: 104-136.
565 Tyson, G.W., Chapman, J., Hugenholtz, P., Allen, E.E., Ram, R.J., Richardson, P.M.
566 et al. (2004) Community structure and metabolism through reconstruction of microbial
567 genomes from the environment. *Nature* **428**: 37-43.
568 Venter, J.C., Remington, K., Heidelberg, J.F., Halpern, A.L., Rusch, D., Eisen, J.A. et

569 al. (2004) Environmental genome shotgun sequencing of the Sargasso Sea. *Science*
570 **304**: 66.
571 Wan, D., Ye, T.H., Lu, Y., Chen, W.L., Cai, P., and Huang, Q.Y. (2019) Iron oxides
572 selectively stabilize plant-derived polysaccharides and aliphatic compounds in
573 agricultural soils. *Eur J Soil Sc* **0**.
574 Ward, L.M., and Shih, P.M. (2019) The evolution and productivity of carbon fixation
575 pathways in response to changes in oxygen concentration over geological time. *Free*
576 *Radic Biol Med* **140**: 188-199.
577 Wood, H.G., Ragsdale, S.W., and Pezacka, E. (1986) The acetyl-CoA pathway: a
578 newly discovered pathway of autotrophic growth. *Trends Biochem Sci* **11**: 14-18.
579 Wu, J., and O'Donnell, A.G. (1997) Procedure for the simultaneous analysis of total
580 and radioactive carbon in soil and plant materials. *Soil Biol Biochem* **29**: 199-202.
581 Wu, X., Ge, T., Wang, W., Yuan, H., Wegner, C.E., Zhu, Z. et al. (2015) Cropping
582 systems modulate the rate and magnitude of soil microbial autotrophic CO2 fixation in
583 soil. *Front Microbiol* **6**: 379.
584 Wu, X., Ge, T., Yuan, H., Li, B., Zhu, H., Zhou, P. et al. (2014) Changes in bacterial
585 CO_2 fixation with depth in agricultural soils. *Appl Microbiol Biol* **98**: 2309-2319.
586 Xiao, K.-Q., Nie, S.-A., Bao, P., Wang, F.-H., Bao, Q.-L., and Zhu, Y.-G. (2014a)
587 Rhizosphere effect has no effect on marker genes related to autotrophic CO_2 fixation
588 in paddy soils? *J Soils Sediments* **14**: 1082-1087.
589 Xiao, K.-Q., Bao, P., Bao, Q.-L., Jia, Y., Huang, F.-Y., Su, J.-Q., and Zhu, Y.-G.
590 (2014b) Quantitative analyses of ribulose-1,5-bisphosphate carboxylase/oxygenase

(RubisCO) large-subunit genes (*cbbL*) in typical paddy soils. *FEMS Microbiol Ecol* **87**: 89-101.

Xiao, K.-Q., Li, L.-G., Ma, L.-P., Zhang, S.-Y., Bao, P., Zhang, T., and Zhu, Y.-G. (2016a) Metagenomic analysis revealed highly diverse microbial arsenic metabolism genes in paddy soils with low-arsenic contents. *Environ Pollut* **211**: 1-8.

Xiao, K.-Q., Li, B., Ma, L., Bao, P., Zhou, X., Zhang, T., and Zhu, Y.-G. (2016b) Metagenomic profiles of antibiotic resistance genes in paddy soils from South China. *FEMS Microbiol Ecol* **92**.

Yuan, H.-Z., Ge, T.-D., Chen, C.-Y., O'Donnell, A.G., and Wu, J.-S. (2012a) Significant role for microbial autotrophy in the sequestration of soil carbon. *Appl Environ Microbiol* **78**: 2328-2336.

Yuan, H., Ge, T., Chen, C., O'Donnell, A.G., and Wu, J. (2012b) Significant role for microbial autotrophy in the sequestration of soil carbon. *Appl Environ Microbiol* **78**: 2328-2336.

Zarzycki, J., and Fuchs, G. (2011) Coassimilation of organic substrates via the autotrophic 3-hydroxypropionate bi-cycle in *Chloroflexus aurantiacus*. *Appl Environ Microbiol* **77**: 6181.

Zhang, L.-M., Offre, P.R., He, J.-Z., Verhamme, D.T., Nicol, G.W., and Prosser, J.I. (2010) Autotrophic ammonia oxidation by soil thaumarchaea. *Proc Natl Acad Sci U S A* **107**: 17240.

Zhang, T., Shi, X.C., Ding, R., Xu, K., and Tremblay, P.L. (2020) The hidden chemolithoautotrophic metabolism of *Geobacter sulfurreducens* uncovered by

613 adaptation to formate. *ISME J*.

615 **Table and Figure legends**

616

617 **Table 1** Shannon–Wiener index of marker genes associated microbes.

	cbbL	*aclA*	*acsA*	*accA*	*hcd*
LZ	3.43	0.25	2.06	0.59	0.96
JX	3.53	0.07	2.59	0.92	0.79
YT	3.60	0.22	2.41	0.6	0.81
TY-G	3.43	0.09	2.31	0.66	0.86
TY-B	3.45	0.07	2.15	0.51	0.87

618

619 **Table 2**. Correlation of soil properties and marker genes with amounts of ^{14}C-SOC

620 and ^{14}C-MBC in paddy soils after 45 d incubation.

	^{14}C-SOC	**^{14}C-MBC**
Soil properties		
pH	0.23	0.03
Total C	-0.76	0.76
Total N	-0.75	0.54
SOC	-0.73	0.78
DOC	-0.02	0.70
Total Fe	0.93*	-0.25
Total Mn	0.79	0.20
clay	0.93*	-0.27
silt	-0.80	0.08
sand	-0.90*	0.59
Gene abundance		
cbbL	0.90*	-0.36
aclA	-0.65	-0.38
acsA	0.37	-0.26
accA	0.23	-0.68
hcd	0.05	-0.81

621 *Correlation is significant at the 0.05 level (2-tailed).

622

Fig. 1 Abundances of marker genes of six autotrophic pathways in five paddy soils from South China, (a) abundance ppm, one read in one million reads, error bars indicate the standard deviation of the mean (n = 2), (b) relative abundance percentages (%) of five marker genes. *cbbL* (ribulose-bisphosphate carboxylase large chain), *aclA* (ATP-citrate lyase alpha-subunit), *acsA* (carbon-monoxide dehydrogenase catalytic subunit), *accA* (acetyl-CoA carboxylase carboxyl transferase subunit alpha), *hcd* (4-hydroxybutyryl-CoA dehydratase). LZ, Leizhou in Guangdong Province; JX, Jiaxing in Zhejiang Provicne; YT, Yingtan in Jiangxi Province; TY-G, Gushi of Taoyuan in Hunan Province; TY-B, Baodongyu of Taoyuan in Hunan Province. Abbreviations apply to all figures and tables in the followings.

Fig. 2 Network of co-occurring autotrophic microbes (genera) of six pathways in paddy soils based on correlation analysis. The size of each node is proportional to the number of connections (that is, degree), and the colors of nodes denote microbes from different pathways: the Calvin cycle (I), the reductive tricarboxylic acid (rTCA) cycle (II), the reductive acetyl-CoA pathway (III), the 3-hydroxypropionate / malyl-CoA cycle (IV) and the 4-hydroxybutyrate cycle (V). The width of each edge is proportional to the weight and the colors of edge denote positive (pink) or negative (light blue) connection.

Fig.3 The amounts of ^{14}C-SOC, ^{14}C-MBC (a) and the synthesis rates of ^{14}C-SOC (b) in five paddy soils incubated in a growth chamber with $^{14}CO_2$ for 45 d. Error bars indicate the standard error of the mean (n = 4) and means with the same letter are not significantly different among different soils ($P > 0.05$).

Fig. 4 Fractionation of soil organic carbon (SOC) in five paddy soils, (a) distribution of SOC and ^{14}C-SOC in different sizes of soil aggregates, (b) distribution of SOC and

651 ^{14}C-SOC in different chemical fractions of soil, HM for humins, HA for humic acids and
652 FA for fulvic acids.

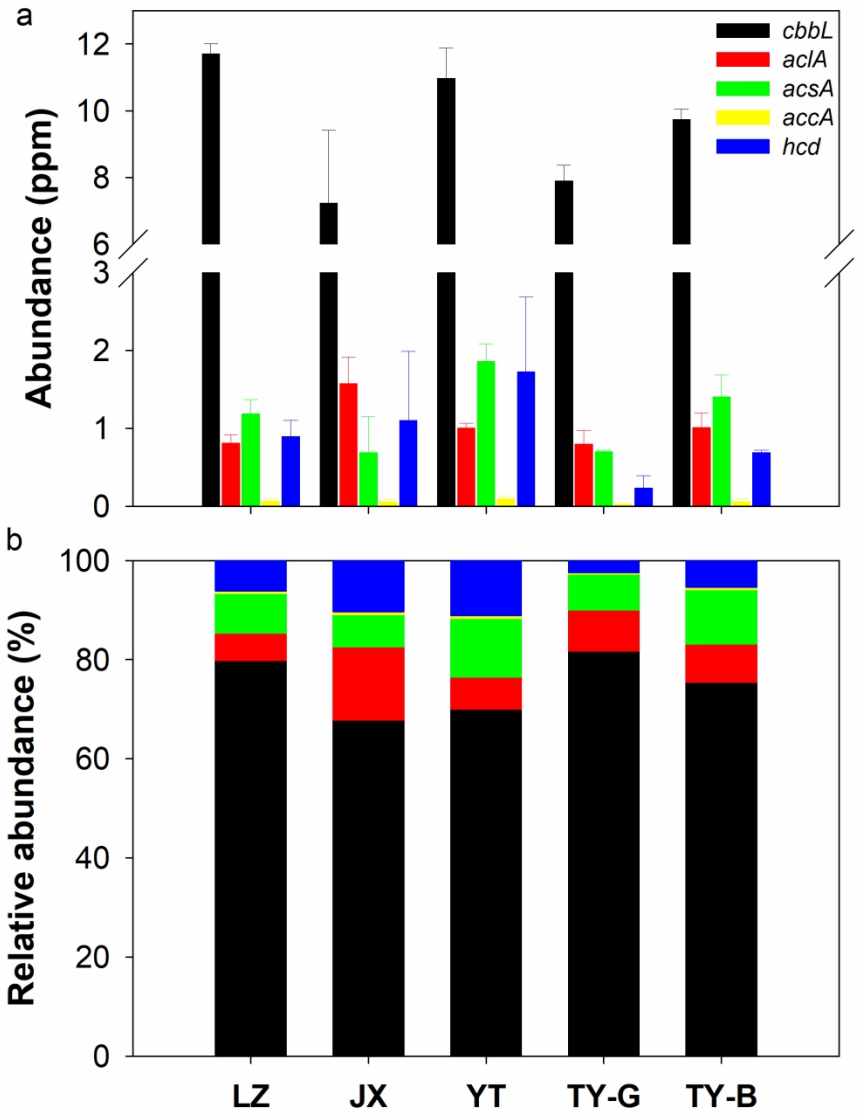

Fig. 1

172x215mm (300 x 300 DPI)

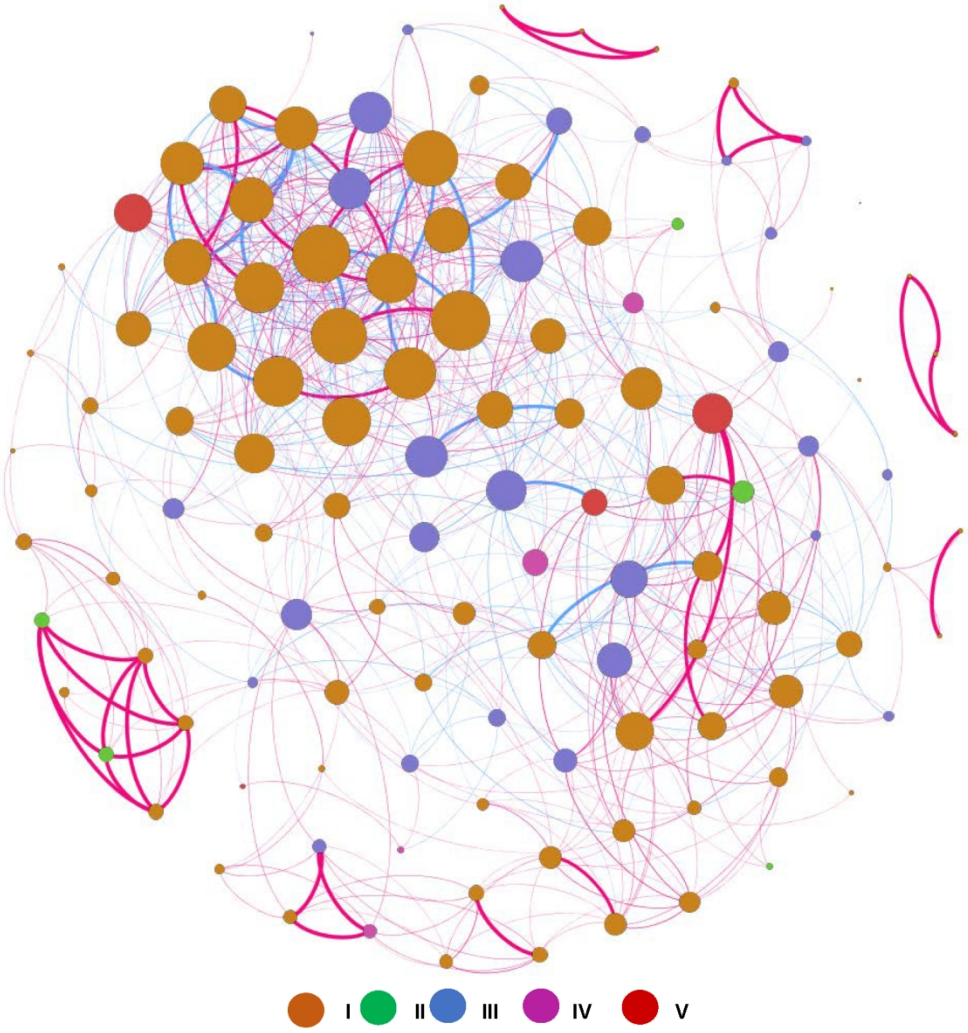

Fig. 2

143x149mm (300 x 300 DPI)

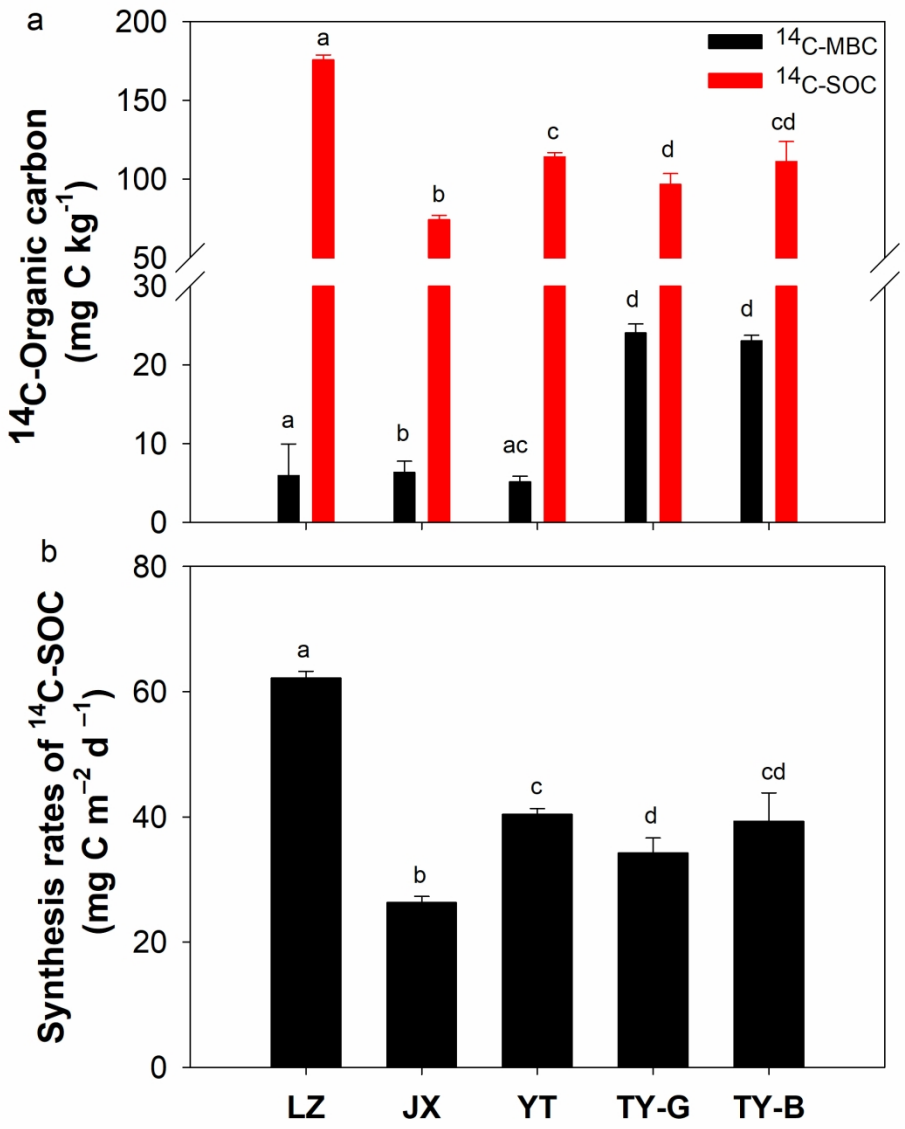

Fig. 3

167x215mm (300 x 300 DPI)

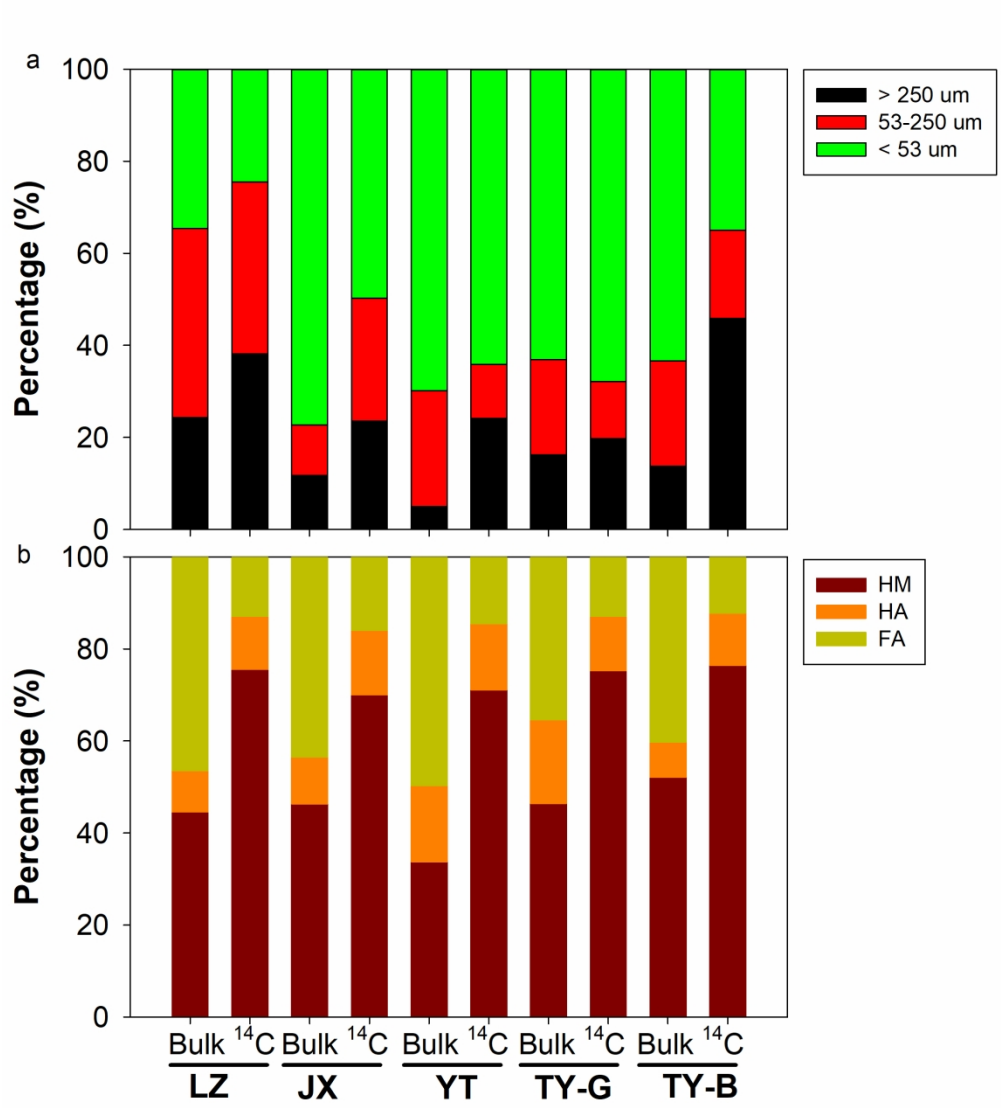

Fig. 4

193x214mm (300 x 300 DPI)